Nature Environment and Pollution Technology
An International Quarterly Scientific Journal

p-ISSN: 0972-6268
(Print copies up to 2016)
e-ISSN: 2395-3454

Vol. 21 | No. 2 | pp. 909-919 | 2022

Original Research Paper

https://doi.org/10.46488/NEPT.2022.v21i02.054

Open Access Journal

Numerical Simulations of Soil Salt Transport in the Irrigation Area of Lower Reaches of Yellow River

Xianqi Zhang*(**)(***) and Peng Chen*†
*School of Water Conservancy, North China University of Water Resources and Electric Power, Zhengzhou 450046, China
**Collaborative Innovation Center of Water Resources Efficient Utilization and Protection Engineering, Zhengzhou 450046, China
***Technology Research Center of Water Conservancy and Marine Traffic Engineering, Henan Province, Zhengzhou 450046, China
†Corresponding author: Peng Chen: 632642579@qq.com

Nat. Env. & Poll. Tech.
Website: www.neptjournal.com

Received: 17-06-2021
Revised: 10-09-2021
Accepted: 22-09-2021

Key Words:
Yellow river
Irrigation area
Soil salt transport
Simulation
Hydrus

ABSTRACT

This paper presents numerical simulations regarding the transport characteristics of soil salt. It has been recognized in recent years that the growth and output of crops in the irrigation area of the lower reaches of the Yellow River are affected by the decreased fertility of soil as a result of the transport of soil salt, due to the long-term farming, fertilization of farmland which contains a high proportion of sands. Accordingly, numerical simulations by Hydrus are carried out, in which, based on the similarity principle, two-dimensional convection-diffusion partial-differential governing equations of unsteady flow in saturated-unsaturated porous media are applied to depict the motion parameters' spatial variability of soil water in the irrigation area. And the van Genuchten equation is adopted to express the relationship between volumetric water content and soil hydraulic conductivity and negative soil water pressure. The irrigation basin of the People's Victory Canal, which is downstream of the Yellow River, is investigated in detail as an example. The findings revealed that soil salt in the irrigation region is transferred by water diffusion, with irrigation and fertilization being the primary causes of downward migration and salt accumulation. It benefits the soil in irrigation areas and protects groundwater.

INTRODUCTION

The irrigation area of the lower reaches of Yellow River goes across the North China Plain, ranging from the east of Qin River mouth to the west of Yellow River estuary, and covers 85 counties in 16 districts (cities) of Henan and Shandong provinces, serving as China's primary base of the grain production, and having played a key role in ensuring the national food security. In this area, the water resources per mu are quite limited as well as difficult to develop and utilize, making flows coming from the Yellow River important water sources for agricultural production. Large-scale agricultural irrigation originated in the 1860s, the average annual water usage was about 12 billion m^3, accounting for 20.7% of the annual runoff of the Yellow River. After running for more than 60 years, massive irrigation with hyper-concentrated Yellow River water, in addition to an irrational system for the development and utilization of regional water resources, and the backwardness in irrigation approaches and technology, leads to variation in the state of the groundwater system and soil salt transport in the irrigation areas. This results in the evolution of water ecology and environment, the soil desertification and decline in the productivity, and the increase of potential secondary salinization, which subsequently affect the sustainable and healthy development of agriculture and the national economy in the downstream irrigation areas (Phogat et al. 2011, Yakirevich et al. 2013, Geng & Boufadel 2015, Sabri et al. 2012).

Investigations concerning the simulations of the salt transport in the irrigation areas have been extensively carried out and productive results have been obtained in recent years (Ramos et al. 2011) Theoretical study of soil salt transport was initially based on Darcy's law which depicts that motion of the salt transport is primarily governed by patterns of the water motion and the salt dissolution (Maziar et al. 2010). Based on Fick's first law, Gardner and Bresler derived the one-dimensional soil solute transport equation. R.Nielsen, Van. Genuchten etc. proposed a movable-immovable water model based on physical nonequilibrium transport models. A series of models developed by the U.S. Salinity Laboratory, for instance, SWMS, HYDRUS, etc., have been widely applied, contributing to fairly good simulations in solute transport in the saturated-unsaturated porous media.

Moreover, Ye (1990) analyzed soil salinity dynamics under infiltration conditions through the simplified transfer function model. Yao and Zhu (2001) established a model of soil salt accumulation and transport under the condition of evapotranspiration. Hu and Gao (2002) constructed a soil transport model and explored the characteristics of salt transport in inland drought regions, according to the principle of water-salt balance. By combining experimental investigations with theoretical analyses, Luo et al. (2008) simulated the salt transport of the cumulated infiltration and the drip irrigation from a point source. Besides, a large number of Chinese researchers utilized SWMS, HYDRUS, and other models to simulate the salt transport in some particular regions (Joseph et al. 2015, Jiang et al. 2011, Dabach et al. 2013, Nachabe et al. 1999). Consequently, a series of valuable results have been obtained regarding simulations of salt transport under various circumstances, for example, the stages for crops' growth, different soil structures, irrigation systems, etc., having laid a solid foundation for further investigations (Chekirbane et al. 2015, Luo et al. 2013, Selim et al. 2013, Morales et al. 2014, Ramos et al. 20110).

It is widely accepted that the properties of soil salt transport, in principle, are complex and vary with multiple factors including not only its concentration gradient, soil properties, plant characteristics, etc., but also the patterns of regional irrigation, tillage, fertilization, and the variations of groundwater, etc. (Medved & Cerny 2015, Comina et al. 2011, Clemente et al. 1997, Russo et al. 2015, Chen et al. 2014). Characterized by its unique nature, geology, groundwater environment, and farming conditions, and combined with the impact of irrigation patterns and planting structures, the downstream irrigation areas of Yellow River significantly differ from other areas in terms of the characteristics of soil salt transport. Thereby, salt transport in the particular areas was simulated to reveal the underlying mechanism and the corresponding migration process. The investigations and results presented in the paper may serve as a theoretical basis and technical support for soil improvement, water-saving irrigation, and the sustainable use of water and land resources in the downstream irrigation areas of the Yellow River.

MATERIALS AND METHODS

Research Method

At the field scale in the irrigation area, the physical and chemical properties of soil are important factors that affect water leakage and salt leaching to different degrees in the horizontal and vertical directions. Besides, the process of soil salt transport is complex and affected by multiple factors, such as soil moisture content, the interaction between salt and soil, salt transformation, root absorption, and so on. Generally, the motion of soil salt is primarily motivated by interactions of convection and hydrodynamic diffusion. The convection-diffusion equation is thereby widely used in describing the dynamical distributions of soil salt, based on which the problems, challenging for some field trials, may also be solved.

Parameters of the Water Motion in Soil

The movement of water in soil generally follows Darcy's law and satisfies the principle of conservation of mass (the continuity equation), based on which the soil water movement can thus be yielded. The soil hydraulic conductivity K is a function of soil moisture content or negative soil water pressure, and specific moisture capacity (water capacity) C is negative reciprocally of the slope of the soil moisture characteristic curve (SMC) at a particular moisture content θ. Empirical formulae based on experimental data are widely used when describing the relationship between negative soil water pressure h, moisture content θ, and soil hydraulic conductivity K due to their complexity. The relevant relationship represented by the modified van Genuchten equation is shown in Fig. 1.

$$\theta(h)=\begin{cases}\theta_a+\dfrac{\theta_m-\theta_a}{(1+|\alpha h|^n)^m} & h<h_s\\ \theta_s & h\ge h_s\end{cases} \quad \ldots(1)$$

$$K(h)=\begin{cases}K_sK_r(h) & h\le h_k\\ K_k+\dfrac{(h-h_k)(K_s-K_k)}{h_s-h_k} & h_k<h<h_s\\ K_s & h\ge h_s\end{cases} \quad \ldots(2)$$

Where,

$$K_r=\frac{K_k}{K_s}\left(\frac{S_e}{S_{ek}}\right)^{1/2}\left[\frac{F(\theta_r)-F(\theta)}{F(\theta_r)-F(\theta_k)}\right]^2 \quad \ldots(3)$$

$$F(\theta)=\left[1-\left(\frac{\theta-\theta_a}{\theta_m-\theta_a}\right)^{1/m}\right]^m \quad \ldots(4)$$

$$m=1-1/n,\ n>1 \quad \ldots(5)$$

$$S_e=\frac{\theta-\theta_r}{\theta_s-\theta_r} \quad \ldots(6)$$

$$S_{ek}=\frac{\theta_k-\theta_r}{\theta_s-\theta_r} \quad (7)$$

$$h_s=-\frac{1}{\alpha}\left[\left(\frac{\theta_s-\theta_a}{\theta_m-\theta_a}\right)^{-1/m}-1\right]^{1/n} \quad \ldots(8)$$

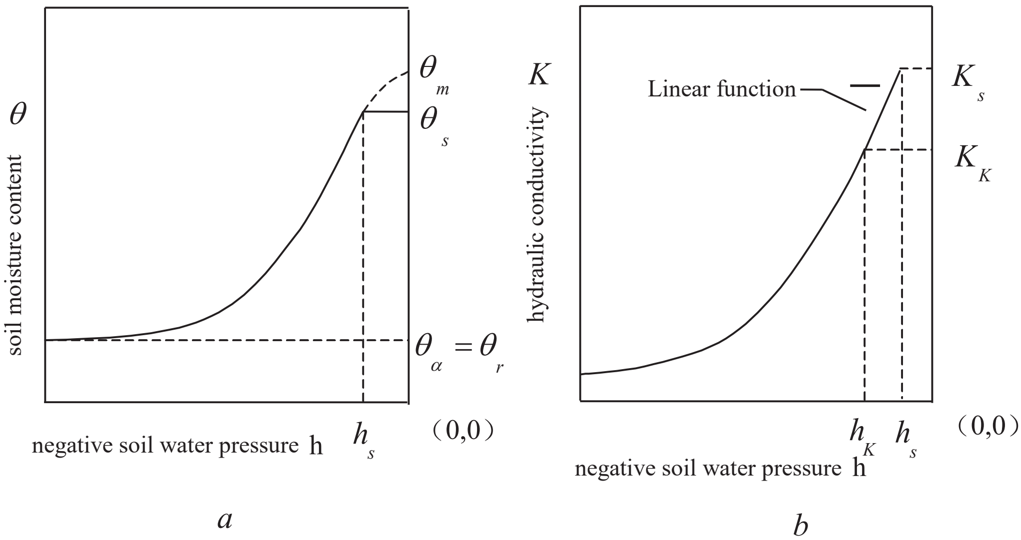

Fig. 1: Relationship between soil moisture and soil hydraulic conductivity and soil negative pressure.

$$h_k = -\frac{1}{\alpha}\left[\left(\frac{\theta_k - \theta_a}{\theta_m - \theta_a}\right)^{-1/m} - 1\right]^{1/n} \quad \ldots(9)$$

Where, θ_r is the residual volumetric water content, i.e., the maximum molecular moisture holding capacity) $[L^3L^{-3}]$, θ_s is saturated volumetric water content $[L^3L^{-3}]$, K_r is the relative unsaturated hydraulic conductivity, K_s is the saturated hydraulic conductivity $[LT^{-1}]$, S_e is the saturation; θ_a with initial setting $\theta_a = \theta_r$ and θ_m are two values assumed to be on the curve of SMC (between negative soil water pressure and hydraulic conductivity), and α, m are empirical constants.

Soil solute transport equation

The two-dimensional convection-diffusion partial differential governing equation for unsteady flow in saturated/unsaturated porous media is,

$$\frac{\partial \theta c}{\partial t} + \frac{\partial \rho s}{\partial t} = \frac{\partial}{\partial x_i}\left(\theta D_{ij}\frac{\partial c}{\partial x_j}\right) - \frac{\partial q_i c}{\partial x_i} + \mu_w \theta c +$$

$$\mu_s \rho s + \gamma_w \theta + \gamma_s \rho - Sc_s \quad \ldots(10)$$

in which c is the solute concentration of soil solution $[ML^{-3}]$, s is the concentration of solid solute adsorbed onto soil particles, ρ is the soil bulk density $[ML^{-3}]$, q_i is the Darcy velocity along the direction x_i $[LT^{-1}]$, μ_w and μ_s are the rate constants for the first-order reaction of liquid and solid solute $[T^{-1}]$, γ_w and γ_s are rate constants for the zero-order reaction of liquid solute $[ML^{-3}T^{-1}]$ and solid solute $[T^{-1}]$, S represents the source/sink term, c_s is the solute concentration of source/sink term $[ML^{-3}]$, D_{ij} is hydrodynamic dispersion coefficient for saturated-unsaturated water $[L^2T^{-1}]$.

The adsorption isotherm model is used for calculation, and the concentration of solute and solid solute adsorbed onto soil particles c, s satisfy

$$s = kc \quad \ldots(11)$$

in which k is the empirical soil adsorption coefficient $[L^3M^{-1}]$.

In saturated-unsaturated porous media, the continuity equation for isothermal Darcy flow can be expressed as,

$$\frac{\partial \theta}{\partial t} = -\frac{\partial q_i}{\partial x_i} - S \quad \ldots(12)$$

Substituting Eq.(11),(12) to Eq. (9), it is yielded

$$-\theta R\frac{\partial c}{\partial t} - q_i\frac{\partial c}{\partial x_i} + \frac{\partial}{\partial x_i}\left(\theta D_{ij}\frac{\partial c}{\partial x_j}\right) + Fc + G = 0, \quad \ldots(13)$$

In which

$$F = \mu_w\theta + \mu_s\rho k + S$$
$$G = \gamma_w\theta + \gamma_s\rho - Sc_s \quad \ldots(14)$$

where R is the Delay factor

$$R = 1 + \frac{\rho k}{\theta} \quad \ldots(15)$$

Moisture content θ and Darcy flow rate q_i can be obtained from the water flow equation so that a solution to Eq. (13) is obtained.

Parameter Calibration

HYDRUS-2D is used to simulate the characteristics of soil salt transport, where the soil in the spatial distribution is inhomogeneous and allows variability. According to the similarity principle proposed by Miller and Simmons, the spatial variability of motion parameters of water in unsaturated soil within infiltration areas is described by calibration factors during simulation. That is to say, an appropriate scale factor is carefully selected so that the relationship between $\theta(h)$ and $K(h)$, of property of spatial variability, can be calibrated and thereafter changed into a relationship between $\theta^*(h^*)$ and $K^*(h^*)$ which is applicable throughout the soil areas. As a consequence, the updated and homogeneous formula for the relationship after parameter calibration can describe the old inhomogeneous relationships in space. The linear model in which the spatial variability of soil water motion is defined by introducing three independent calibration coefficients is,

$$\begin{aligned} K(h) &= \alpha_K K^*(h^*) \\ \theta(h) &= \theta_r + \alpha_\theta\left[\theta^*(h^*) - \theta_r^*\right], \\ h &= \alpha_h h^* \end{aligned} \quad \ldots(16)$$

Where, α_θ, α_h and α_K are, respectively, calibration coefficients of moisture content, negative soil water pressure, and hydraulic conductivity. In most cases, these three coefficients are independent, while being dependent on each other in some specific cases. In an initial situation, $\alpha_\theta = 1$, within the meanwhile, and $\alpha_K = \alpha_h^{-2}$. The parameters for solute transport include longitudinal dispersion coefficient D_L, lateral dispersion coefficient D_T, molecular diffusion coefficient NO_3^--N in free water D_w, mineralization rate of organic nitrogen k_{min}, biological immobilization rate k_{im} NO_3^--N, and k_{den} denitrification rate NO_3^--N.

CASE STUDY

Description of the Irrigation Areas Studied

People's Victory Canal is one of the important irrigation areas the downstream of Yellow River, with longitude and latitude respectively of 113°31'-114°25' E and35°0'-35°30'N, whose boundaries reach Yellow River to the south, Wei River to the north, Communistic Canal to the west, and Red Flag Main Canal to the east. Most parts of the irrigation areas are plains resulting from erosion, flooding, and siltation of the Yellow River, where moisture soils account for 75%, aeolian sandy soils 12.5%, and solonchak-like soils 8%. The irrigation area has a warm temperate continental monsoon climate with 4 distinct seasons, where spring is relatively dry, summer windy with frequent rainfall, and autumn of crisp air, and being beneficial for the crops' growth with an annual rainfall of around 550-670 mm. The primary economic crops planted are wheat, rice, peanuts, cotton, etc. The farming patterns produce two crops a year, with wheat planted in winter while shifted to corn, peanuts, and rice in summer. Since 1952 when the irrigation area was completed, it covers, in total, 47 townships (towns) and 973 villages, with an overall population of 265.4 million. Besides, its average annual quantity of water drawing from the Yellow River amounts to 378 220 000 m^3, and the irrigation area amounts to 1422 km^2. It thus has become one of the main regions for China's Grain Production.

Soil Hydraulic Parameters

The soil of the People's Victory Canal is primarily silt loam. Considering the impact of spatial variability of soil hydraulic parameters on salt leaching at the field scale, the effect of soil hydraulic parameters of different degrees of spatial variability on the leaching NO_3^--N is to be studied, where the degrees of variability are determined based on the following criterion: weak variability is assumed when the coefficient of variation $C_V < 0.1$, while moderate as $0.1 < C_V < 1$; and it is assumed that soil clay, silt, and soil bulk density follow the normal distribution. During the simulations by Hydrus-2D, the Monte Carlo method is used to randomly generate a certain number of soils with weak and moderate variability. The corresponding soil hydraulic parameters are thereafter obtained by the program Rosetta. The van Genuchten-Mualem model is used to describe parameters of the characteristic curve for soil moisture and unsaturated hydraulic conductivity. Parameters for solute transport, such as D_L, D_T, D_W, k_{min}, k_{im} and k_{den} which are defined previously, are obtained via field experiments, monitoring, and empirical formulae. When simulating the migration of nitrate ions underground under natural conditions within a year, radiation, temperature, humidity, and other meteorological data are inputs to interpret rainfall from the upper boundary, and the potential evapotranspiration ETP can be automatically calculated according to the Penman-Monteith equation defined within the model.

Case Settings

The variations of nitrate compounds in the irrigation areas are significant, primarily resulting from excessive fertilization and flooding irrigation during agricultural production. In terms of salt transport simulation of groundwater in the irrigation regions, the main attention is paid to the transport process of nitrate. The data concerning weather conditions used for simulation is based on monitoring data published by the small weather stations and China Meteorological Administration, and parameters concerning the soils and irrigation status are determined according to field investigations, monitoring data, and practical production activities in the irrigation area. Two cases to obtain the status of downward migration of nitrate iron are set for the simulations, i.e.

Case *I*: conditions within one week after a process of irrigation and fertilization;
Case *II*: conditions within one year under natural circumstances, more specifically, under natural rainfalls.

RESULTS AND DISCUSSION

Results of the Simulations

When simulating the status of downward migration for nitrate ions within one week after a process of irrigation and fertilization, only salt transport is simulated by referring to variations both in groundwater level and depth of salt transport and ignoring the water uptake of the root. To determine the concentration of irrigation water mixing with fertilizers, it is of priority to refer to the local irrigation quota and actual irrigation conditions in irrigation to conduct generalized conversion. Set the head of the upper boundary fixed, and the lower as free drainage. Model lengths are set with 10m in depth and 5m in width for simulations.

Results Under Case *I*

Figs. 2-9 mainly depicts the transport status of nitrate ion within one week after applying a process of irrigation and fertilization.

Based on the actual situation of the irrigation area, the nitrate ion concentration in water after irrigation and fertilization is 0.07 $M.L^{-3}$. The ions have migrated from the surface downward to a soil depth of 60 cm within 24 h, while the concentration is decreased from top to downward and various zones of ion concentration of different thicknesses are formed at the 24^{th} h.

From the 24^{th} to 168^{th} h, with the immigration of ions continuously heading downwards, zones of different ion concentrations have been moving in the same way and

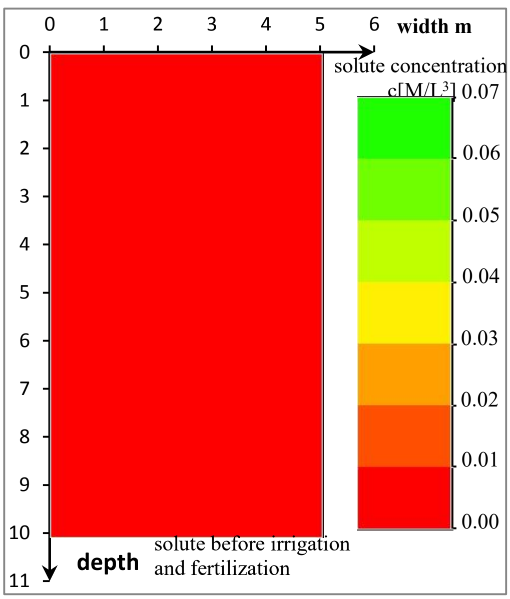

Fig. 2: Before irrigation and fertilization.

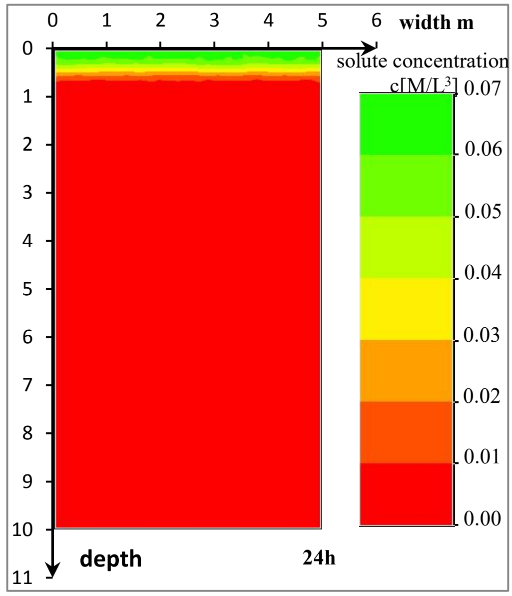

Fig. 3: Nitrate concentration at the 24^{th} h.

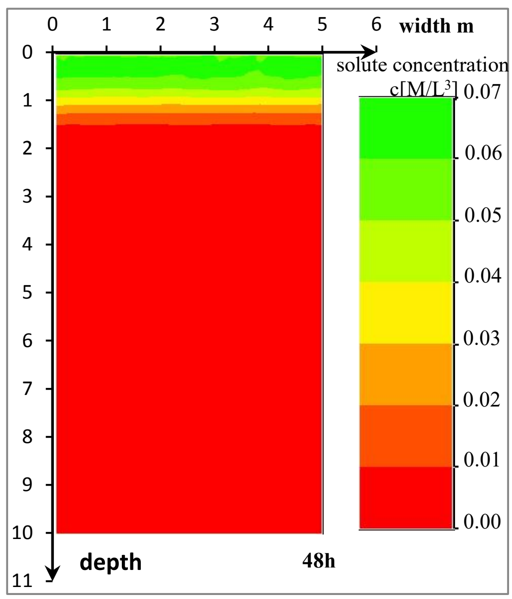

Fig. 4: Nitrate concentration at the 48^{th} h.

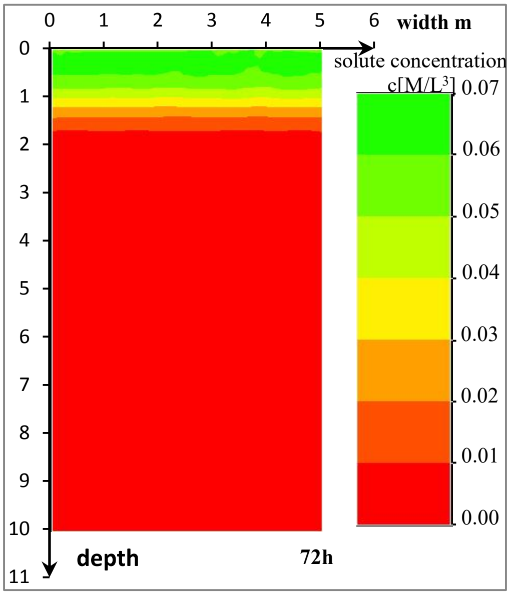

Fig. 5: Nitrate concentration at the 72nd h.

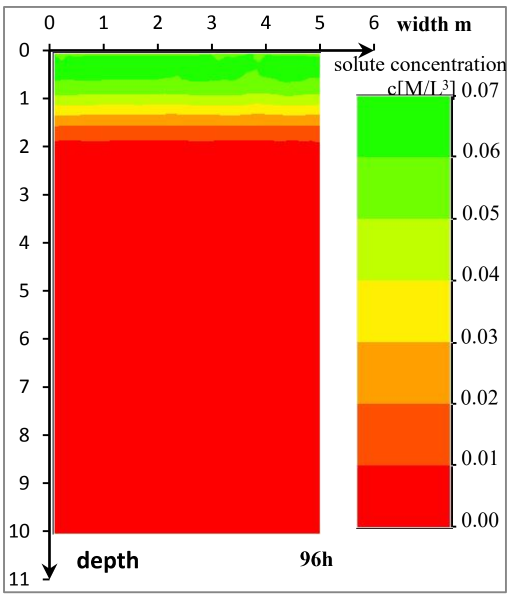

Fig. 6: Nitrate concentration at the 96th hour.

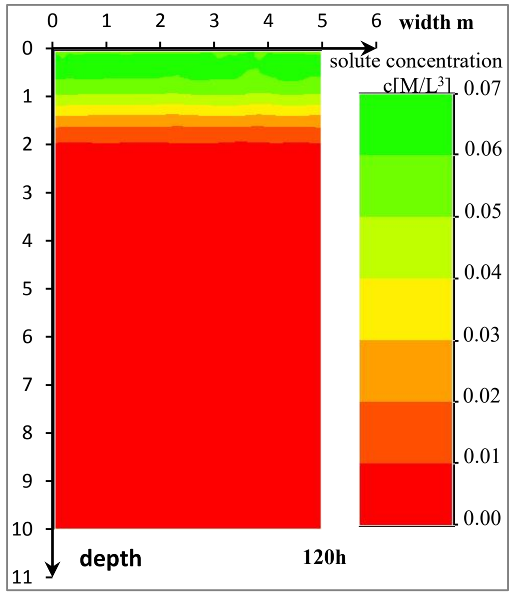

Fig. 7: Nitrate concentration at the 120th hour.

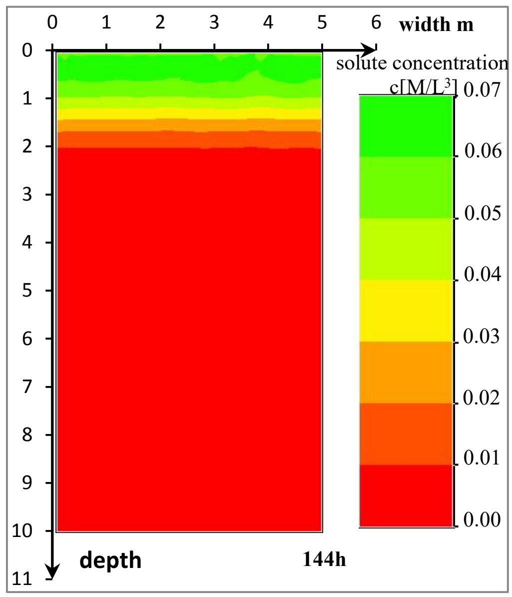

Fig. 8: Nitrate concentration at the 144th hour.

becoming increasingly thick. At the 168th h, the zone of nitrate ions with concentrations ranging from 0.01 M.L^{3}~0.02 M.L^{-3} is moving downward to the depth of 210 cm, and the concentration of ions underneath 98 cm of the ground surface is ranging from 0.05 M.L^{-3}-0.07 M.L^{-3}.

Results of Case *II*

Based on the average meteorological parameters within various years, where the precipitation is low in April and September, and high in May, July, October, and November, the simulated data of average precipitation are close to realistic situations without considering the effect of groundwater on soil moisture content. Figs. 10 to 22 are about the simulated transport of nitrate ions in irrigation soil within one year under natural conditions.

Based on the figures, the downward transport rate of

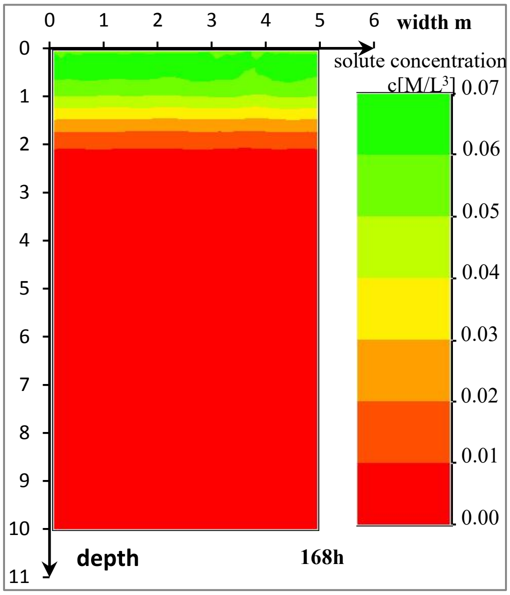

Fig. 9: Nitrate concentration at the 168th hour.

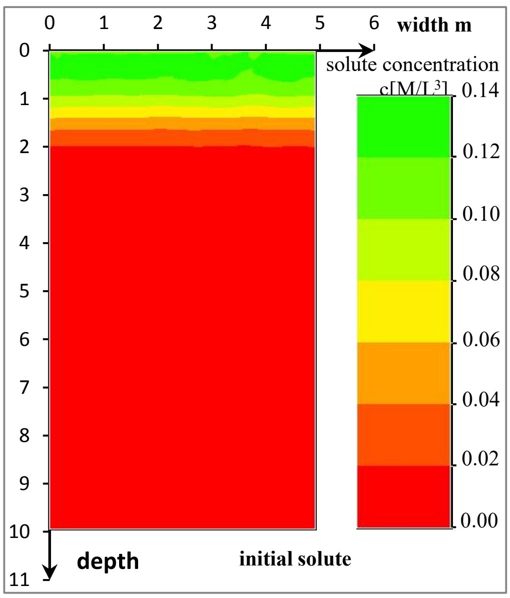

Fig. 10: Initial state of the solute status.

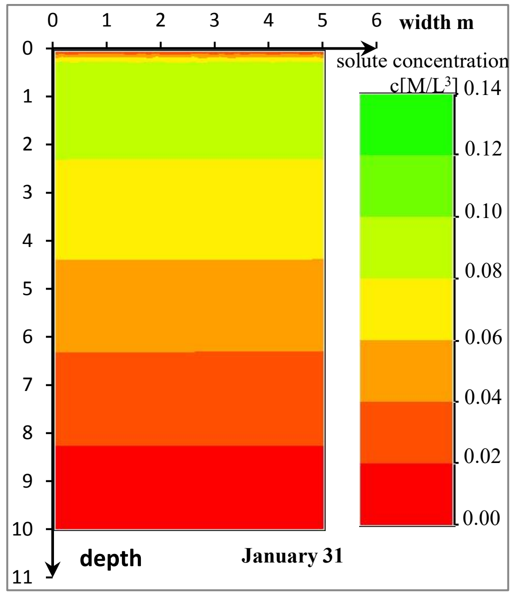

Fig. 11: Solute status on January 31st.

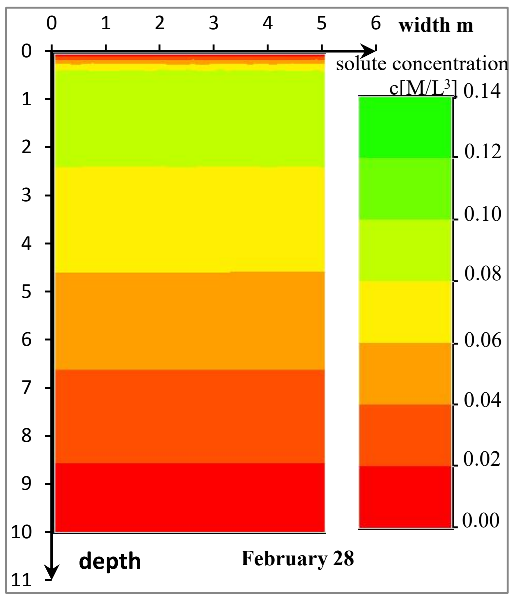

Fig. 12: Solute status on February 28th.

soil nitrate ions is fairly slow without precipitation in January, February and March. Until March 31st, nitrate ions have migrated 5 cm downward from the surface, and the subsurface concentration of nitrate ions at the depths from 5 to 34cm, which increases with depth, has become lower than the initial 0.08M.L^{-3}. Moreover, precipitation in April results in an increased transport rate of the soil nitrate ions. And the downward migration reached a depth of 36 cm on April 30th.

Different levels of precipitation in May, July, September, October, and November have resulted in continuously downward migration of the nitrate ions, subsequently resulting in an increased concentration of nitrate ions in deeper layers. Until December 31st, the transport distance has reached a

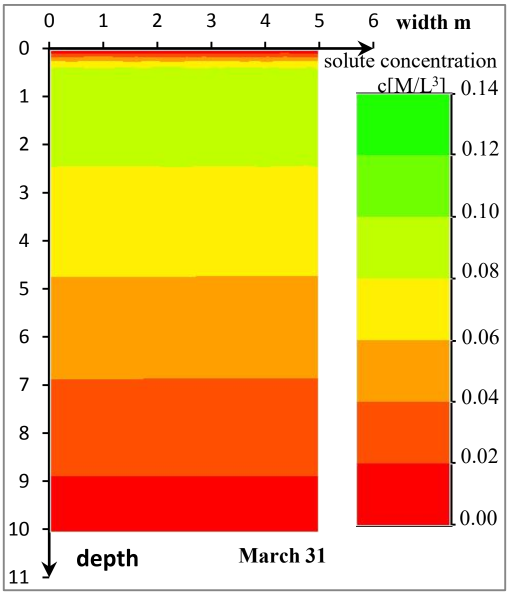

Fig. 13: Solute status on March 31st.

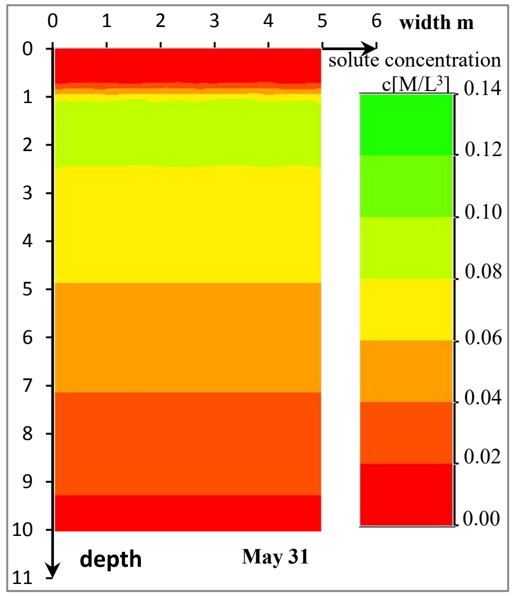

Fig. 15: Solute status on May 31st.

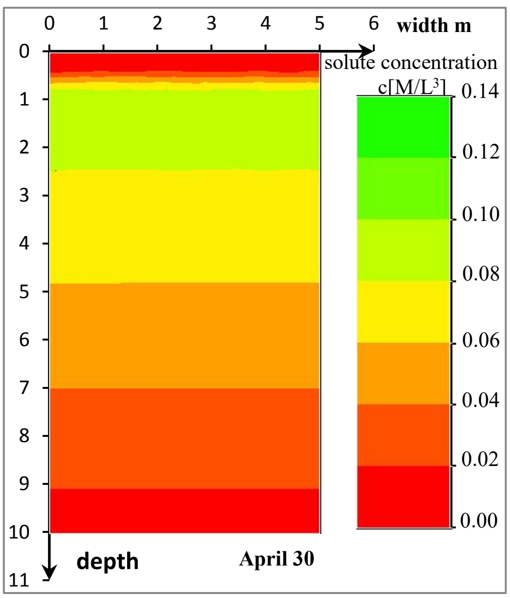

Fig. 14: Solute status on April 30th.

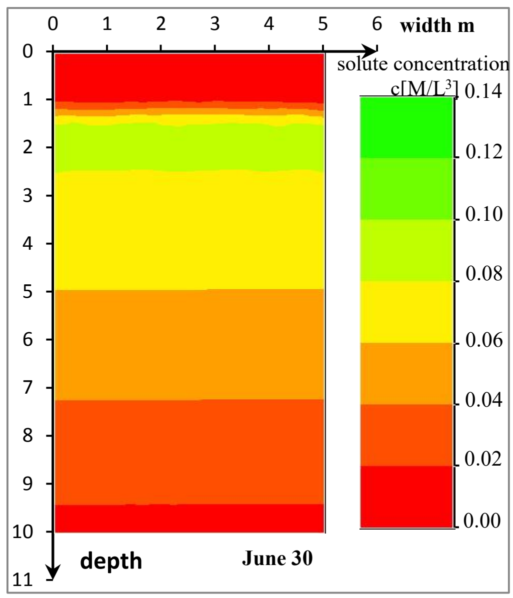

Fig. 16: Solute status on June 30th.

depth of 190 cm.

DISCUSSION

Based on the previous simulations regarding the salt transport of soil in the irrigation area of the People's Victory Canal, it was illustrated that the concentration of nitrate ions decreases with depth while the nitrate ions migrate downward along the soil water. Due to multiple factors, for instance, soil filtration and root absorption of plants, the concentration of nitrate ions in deeper layers does not reach a certain value while soil water transports downward to a certain depth, indicating that the transport of nitrate ions in soil layers lags behind water migration. Moreover, nitrate ions reach deeper layers over time with a decreasing concentration in lower layers as a consequence of different interferences from uptake by crops.

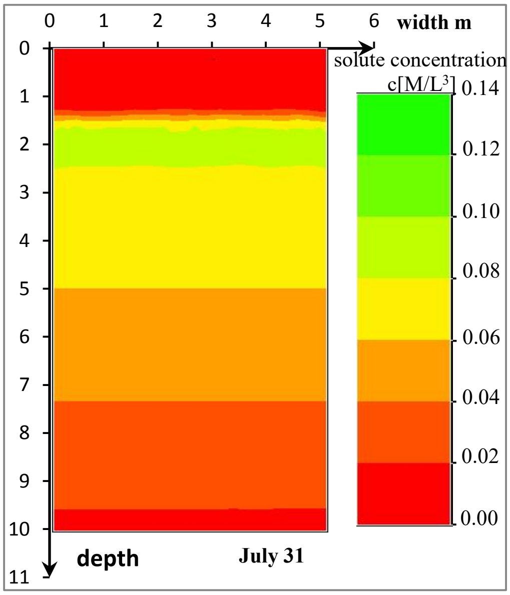

Fig. 17: Solute status on July 31st.

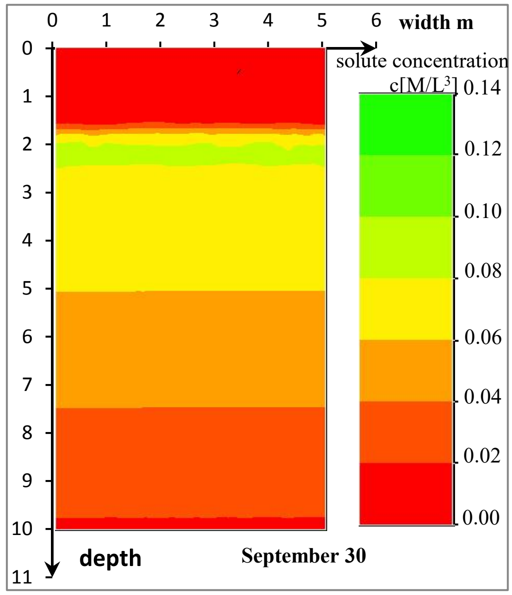

Fig. 19: Solute status on September 30th.

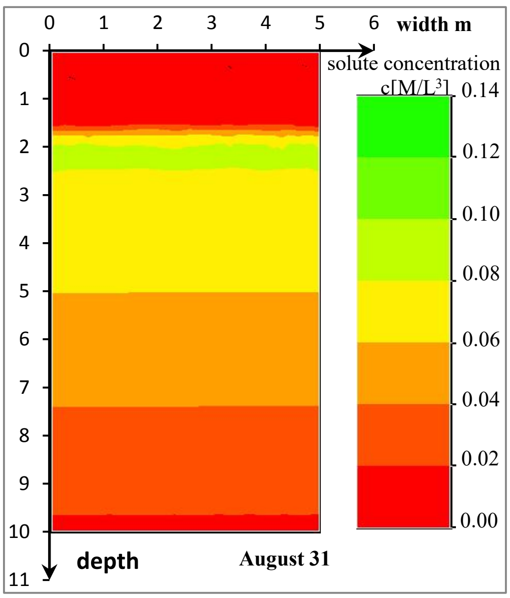

Fig. 18: Solute status on August 31st.

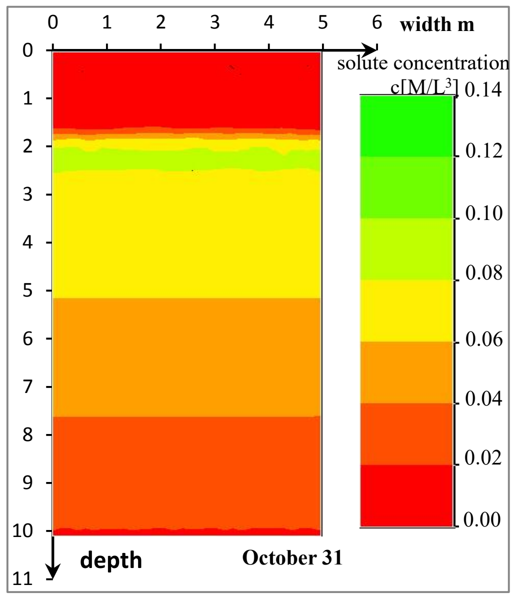

Fig. 20: Solute status on October 31st.

Observation points are set along the direction of soil depth so that variation of salt concentration can be monitored. A brief layout of the observation points is shown in Fig. 23 and the variations of solute concentration at different observation points are depicted in Fig. 24.

As can be seen from Figs. 23 and 24, after a process of irrigation and fertilization, observation point No. 3, being closest to the surface, increases rapidly in salt concentration while remaining steady in concentration after reaching to0.06mg/cm^3 at 12^{th} h. Within one week, the concentrations of nitrate ion at Nos. 1, 4, and 6 points have been gradually increased over time and ultimately become steady. After one week, with no concentration of nitrate ion at No. 2, 5, and 7, the highest concentration appears at No. 3 while the lowest at No. 1, indicating that the salt is mainly concentrated within the depth below point No. 3 and above No.1. Under natural

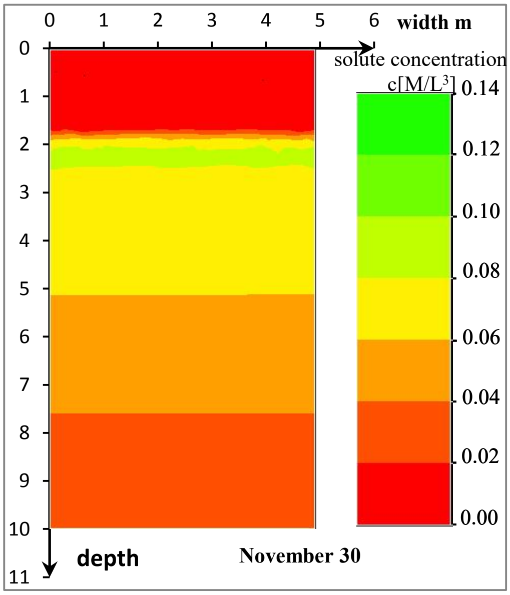

Fig. 21: Solute status on November 30th.

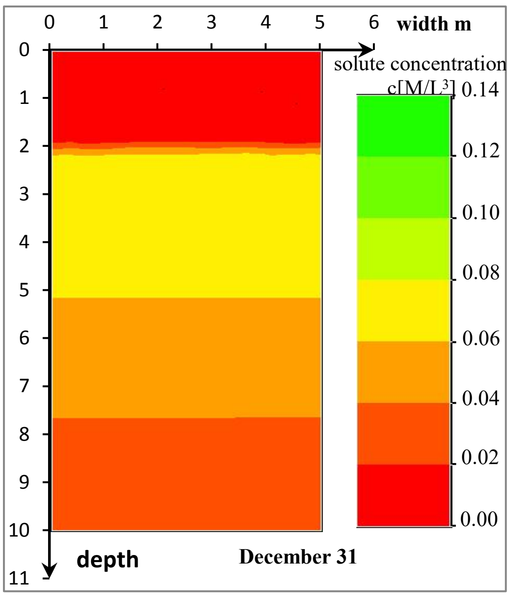

Fig. 22: Solute status on December 31st.

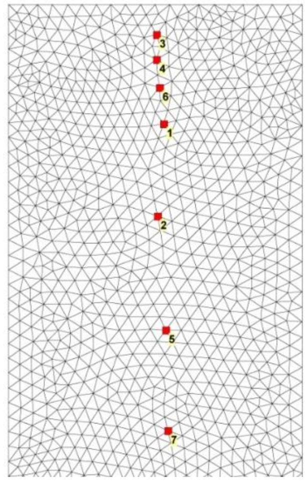

Fig. 23: Layout of the observation points.

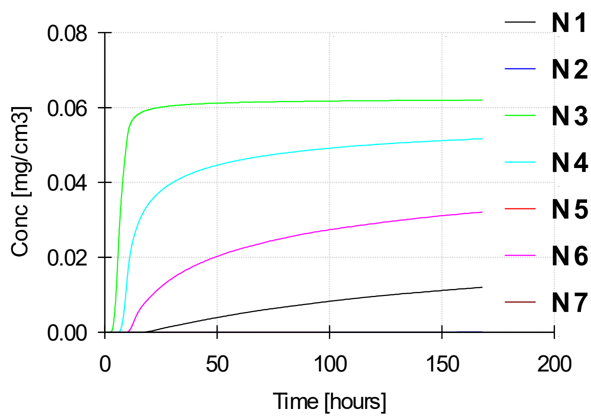

Fig. 24: Variation of concentration at observation points.

precipitation, a certain concentration (or a certain amount) of nitrate ions on the surface may move downwards to deeper soil layers along with the infiltration of natural precipitation, resulting in a continuous increase of nitrate ions concentration in deeper layers. Based on the simulations of natural precipitation, it was indicated that the migration of nitrate ions downwards within a year can reach a depth of 190 cm and cause a continuous increase in the concentration of nitrate ions in deeper layers, which, consequently, may significantly affect the quality of groundwater.

CONCLUSIONS

Based on the two-dimensional convection-diffusion partial differential equations of unsteady flow in saturated-unsaturated porous media and the van Genuchten equation, simulations by Hydrus have been carried out in this paper regarding soil salt transport in the irrigation area of the People's Victory Canal located in the downstream of Yellow River. Results in the present paper illustrate that the salt in the irrigation area migrates downwards along with the diffusion of water in soils, to a depth that increases with the downward depth of the transported water. Meanwhile, a deeper depth tends to be with a lower concentration of soil salt. However, when compared with the situation before irrigation and fertilization, both the rate of transporting downwards and the depth with the same level of concentration of soil salt obviously increase after a process of irrigation and fertilization. Meanwhile, the downward salt, which moves slowly under conditions of surface seepage like natural precipitation, results in a continuous increase of the concentration in deeper layers due to the soil adsorption. Based on the present paper, it is recommended that measures can be taken to strengthen rational management mechanisms for water diversion irrigation, improve irrigation methods and farming patterns in some areas, and apply scientific use of fertilizers, aiming at reducing the transport quantity of salt into the soil, protecting the environmental quality of groundwater, and facilitating sustainable use of soil and water resources in the irrigation area.

ACKNOWLEDGMENT

This work is financially supported by NSFC-Henan Provincial People's Government Joint Fund of Personnel Training (No.U1304511), International cooperation in science and technology project of Henan Province (No.152102410052), Collaborative Innovation Center of Water Resources Efficient Utilization and Protection Engineering, Henan Province, Program for Science & Technology Innovation Talents in Universities of Henan Province(No.15HASTIT049), and Program for Innovative Research Team (in Science and Technology) in University of Henan Province(No.14IRT-STHN028). Our gratitude is also extended to reviewers for their efforts in reviewing the manuscript and their very encouraging, insightful, and constructive comments.

REFERENCES

Chekirbane, A., Tsujimura, M. and Kawachi, A. 2015. 3D simulation of a multi-stressed coastal aquifer, northeast of Tunisia: Salt transport processes and remediation scenarios. Environ. Earth Sci., 73(4): 1427-1442.

Chen, L.J., Feng, Q. and Li, F.R. 2014. A bidirectional model for simulating soil water flow and salt transport under mulched drip irrigation with saline water. Agric. Water Manag., 146: 24-33.

Clemente, R.S., Prasher, S.O. and Bonnell, R.B. 1997. Application of PESTFADE to simulate salt movement in soils. Canad. Water Resour. J., 22(2): 167-184.

Comina, C., Cosentini, R. and Della,V.G. 2011. 3D-electrical resistivity tomography monitoring of salt transport in homogeneous and layered soil samples. Acta Geotech., 6(4): 195-203.

Dabach, S., Lazarovitch, N. and Simunek, J. 2013. Numerical investigation of irrigation scheduling based on soil water status. Irrig. Sci., 31: 27-36.

Geng, X.L. and Boufadel, M.C. 2015. Numerical modeling of water flow and salt transport in bare saline soil subjected to evaporation. J. Hyrdrol., 524: 427-438.

Hu, A.Y. and Gao, J. 2002. Soil water and salt balance model for an irrigation district in the arid and inland region. Adv. Water Sci., 13(6): 726-729 (in Chinese)

Jiang, J., Feng, S.Y. and Huo, Z.L. 2011. Application of the SWAP model to simulate water-salt transport under deficit irrigation with saline water. Math. Comp. Model., 54(3-4): 902-911.

Joseph, M., Subrahmanyam, B. and Ebenezer, S. 2015 Seasonal variability of salinity and salt transport in the northern Indian Ocean. J. Phys. Oceanogr., 45(7): 1947-1966.

Luo, J.F., Hans, J.G. and Lambertus, M.J. 2013. 3D modeling of saline groundwater flow and transport in a flooded salt mine in Stassfurt, Germany. Mine Water Environ., 32(1): 71-77.

Luo, P, Zhang, F.C. and Li, X.J. 2008. Experimental study on the influence of infiltration head on water and salt transportation in saline-alkali soil. Water-Saving Irrig., 6: 4-7 (in Chinese)

Maziar, M, Kandelous, R. and Simunek, J. 2010. Numerical simulations of water movement in a subsurface drip irrigation system under field and laboratory conditions using HYDRUS-2D. Agric. Water Manag., 97(7): 1070-1076.

Medved, I. and Cerny, R.J. 2015. Role of time relaxing in a one-dimensional diffusion-advection model of water and salt transport. Adv. Math. Phys., 35: 307-312.

Morales, I., Atoyan, J.A. and Amador, J.A. 2014. Transport of pathogen surrogates in soil treatment units: Numerical model. Water, 6(4): 818-838.

Nachabe, M.H., Ahuja, L.R. and Butters, G. 1999. Bromide transport under sprinkler and flood irrigation for no-till soil condition. J. Hydrol., 214: 8-17.

Phogat, V., Yadav, A.K., Malik, R.S., Kumar, S. and Cox, J.J. 2011. Simulation of salt and water movement and estimation of water productivity of rice crop irrigated with saline water. Paddy Water Environ., 8(4): 333-346.

Ramos, T.B, Simunek, J., Goncalves, M.C., Martins, J.C., Prazeres, A., Castanheira, N.L. and Pereira, L.S. 2011. Field evaluation of a multicomponent solute transport model in soils irrigated with saline waters. J. Hyrdrol., 407(1-4): 129-144.

Ramos, T.B., Simunek, J. and Goncalves, M.C. 2011. Two-dimensional modeling of water and nitrogen fate from sweet sorghum irrigated with fresh and blended saline waters. Agric. Water Manag., 111: 87-104.

Russo, D., Laufer, A. and Bardhan, G. 2015. Salinity control in a clay soil beneath an orchard irrigated with treated wastewater in the presence of a high water table: A numerical study. J. Hydrol., 531: 198-213.

Sabri, K., Hachicha, M., Bouhlila, R. and Batlle, J.J. 2012. Simulation of water and salts dynamics in Bouhajla (Central Tunisia): Exceptional rainfall effect. Soil Water Res., 7(1):36-44.

Selim, T., Bouksila, F. and Berndtsson, R. 2013. Soil water and salinity distribution under different treatments of drip irrigation. Soil Sci. Soc. Am. J., 77(4): 1144-1156.

Yakirevich, A., Weisbrod, N., Kuznetsov, M., Villarreyes, C.A.R, Benavent Chavez, A.M. and Ferrando, D.J. 2013. Impact of solute recycling on groundwater salinization under irrigated lands: A study of the alto Piura aquifer Peru. J. Hydrol., 482: 25-39.

Yao, D.L. and Zhu, J.S. 2001. Model on water-salt movement and application in the field of arid land. J. Desert Res., 21(3): 286-290 (in Chinese)

Ye, Z.T. 1990. The utilization of the salt transfer function model in studying water-salt movement in soil layers under infiltration. J. Hydraul. Eng., 2: 4-9 (in Chinese)